Lithos 284–285 (2017) 512–524

Contents lists available at ScienceDirect

Lithos

journal homepage: www.elsevier.com/locate/lithos

Recurrent Early Cretaceous, Indo-Madagascar (89–86 Ma) and Deccan (66 Ma) alkaline magmatism in the Sarnu-Dandali complex, Rajasthan: $^{40}Ar/^{39}Ar$ age evidence and geodynamic significance

Hetu Sheth [a,*], Kanchan Pande [a], Anjali Vijayan [a], Kamal Kant Sharma [b], Ciro Cucciniello [c]

[a] Department of Earth Sciences, Indian Institute of Technology Bombay (IITB), Powai, Mumbai 400076, India
[b] Department of Geology, Government Postgraduate College, Sirohi, Rajasthan 307001, India
[c] Dipartimento di Scienze della Terra, dell'Ambiente e delle Risorse (DiSTAR), Università di Napoli Federico II, Complesso Universitario Monte Sant'Angelo, Via Cintia 21 (edificio L), 80126 Napoli (Naples), Italy

ARTICLE INFO

Article history:
Received 20 January 2017
Accepted 8 May 2017
Available online 15 May 2017

Keywords:
Alkaline magmatism
Sarnu-Dandali
Rajasthan
India
$^{40}Ar/^{39}Ar$ geochronology

ABSTRACT

The Sarnu-Dandali alkaline complex in Rajasthan, northwestern India, is considered to represent early, pre-flood basalt magmatism in the Deccan Traps province, based on a single $^{40}Ar/^{39}Ar$ age of 68.57 Ma. Rhyolites found in the complex are considered to be 750 Ma Malani basement. Our new $^{40}Ar/^{39}Ar$ ages of 88.9–86.8 Ma (for syenites, nephelinite, phonolite and rhyolite) and 66.3 ± 0.4 Ma (2σ, melanephelinite) provide clear evidence that whereas the complex has Deccan-age (66 Ma) components, it is dominantly an older (by ~20 million years) alkaline complex, with rhyolites included. Basalt is also known to underlie the Early Cretaceous Sarnu Sandstone. Sarnu-Dandali is thus a periodically rejuvenated alkaline igneous centre, active twice in the Late Cretaceous and also earlier. Many such centres with recurrent continental alkaline magmatism (sometimes over hundreds of millions of years) are known worldwide. The 88.9–86.8 Ma $^{40}Ar/^{39}Ar$ ages for Sarnu-Dandali rocks fully overlap with those for the Indo-Madagascar flood basalt province formed during continental breakup between India (plus Seychelles) and Madagascar. Recent $^{40}Ar/^{39}Ar$ work on the Mundwara alkaline complex in Rajasthan, 120 km southeast of Sarnu-Dandali, has also shown polychronous emplacement (over ≥45 million years), and 84–80 Ma ages obtained from Mundwara also arguably represent post-breakup stages of the Indo-Madagascar flood basalt volcanism. Remnants of the Indo-Madagascar province are known from several localities in southern India but hitherto unknown from northwestern India 2000 km away. Additional equivalents buried under the vast Deccan Traps are highly likely.

1. Introduction

Major tectonic events that led to the final dispersal of East Gondwana include the breakup and separation of India, Seychelles and Madagascar in Late Cretaceous and Palaeocene time (e.g., Norton and Sclater, 1979; Reeves, 2014; Bhattacharya and Yatheesh, 2015; Fig. 1). The oldest among these events is the separation of India and the Seychelles from Madagascar, which was initiated at ~88 Ma (e.g., Bhattacharya and Yatheesh, 2015; Pande et al., 2001; Storey et al., 1995), and created the Mascarene Basin (Fig. 1a,b). This breakup event was immediately preceded by flood basalt volcanism on Madagascar, the oceanic Madagascar Plateau and the Conrad Rise (Storey et al., 1995; Torsvik et al., 1998), with correlatives in southern India (e.g., Pande et al., 2001; Kumar et al., 2001; Radhakrishna and Joseph, 2012) (Fig. 2).

At ~68.5 Ma, India broke up from the welded Seychelles and Laxmi Ridge (referred to as Greater Seychelles), resulting in the formation of the Laxmi Basin between India and the Laxmi Ridge, and the Gop Basin between the Laxmi Ridge and the Saurashtra Volcanic Platform (Fig. 1c). This was in turn followed by the breakup of the Seychelles from the conjoined Laxmi Ridge-India, initiated shortly before chron C28ny (Bhattacharya and Yatheesh, 2015; Chaubey et al., 2002; Collier et al., 2008; Ganerød et al., 2011; Royer et al., 2002; Yatheesh, 2007), i.e., shortly before ~62.5 Ma (in the geomagnetic polarity timescale of Cande and Kent, 1995). This separation created the conjugate Arabian and Eastern Somali basins on the Laxmi Ridge and Seychelles sides, respectively (Fig. 1d), and was preceded by the formation of the Deccan Traps flood basalt province (Fig. 1d) during 66–65 Ma (Baksi, 2014). Post-breakup Deccan magmatism continued up to ~62–61 Ma in both western India and the Seychelles (Ganerød et al., 2011; Owen-Smith et al., 2013; Shellnutt et al., 2017; Sheth and Pande, 2014; Sheth et al., 2001).

The Indo-Madagascar and Deccan flood basalt provinces contain enormous volumes of tholeiitic basalts (e.g., Beane et al., 1986;

* Corresponding author.
E-mail address: hcsheth@iitb.ac.in (H. Sheth).

http://dx.doi.org/10.1016/j.lithos.2017.05.005
0024-4937/

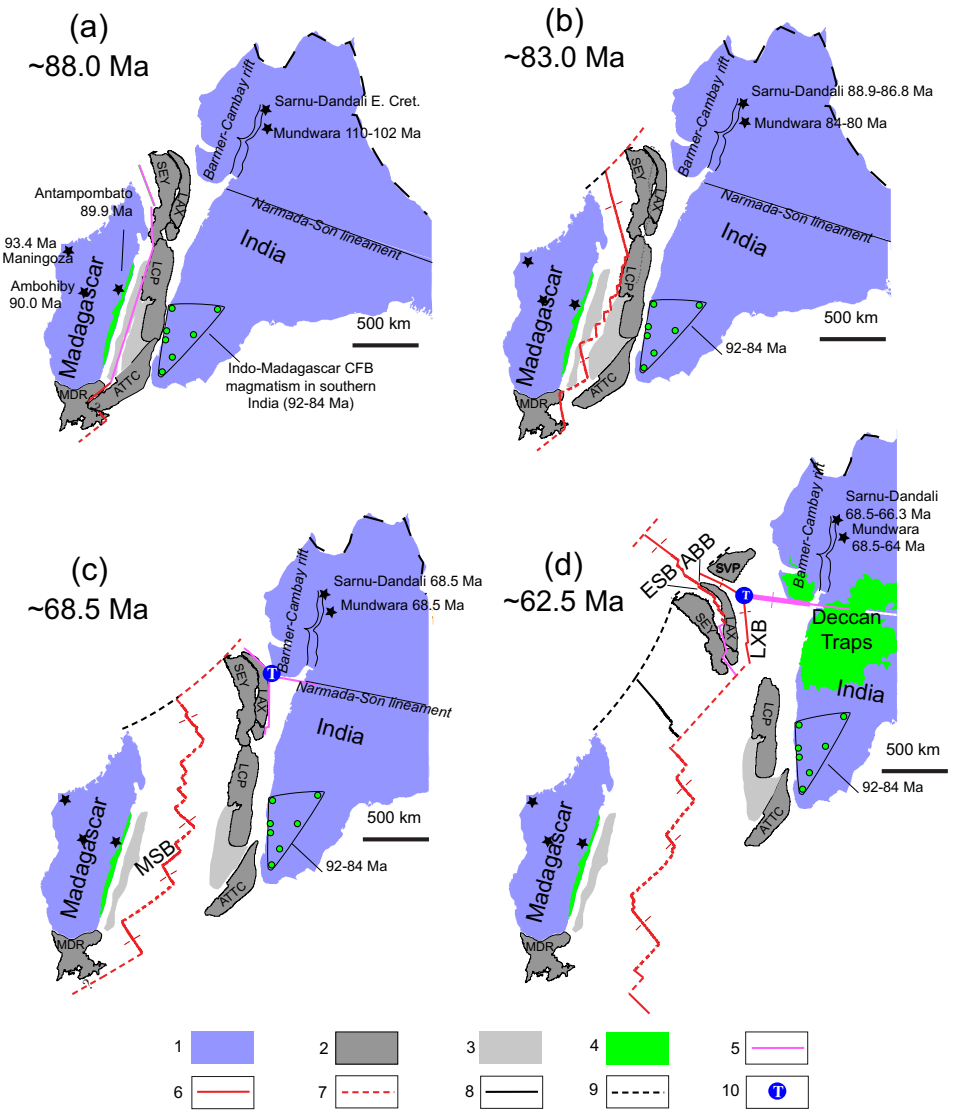

Fig. 1. Schematic diagrams (based on Bhattacharya and Yatheesh, 2015) depicting the major stages of India-Seychelles-Madagascar breakup and the early opening history of the Arabian Sea, for (a) ~88 Ma, (b) ~83.0 Ma, (c) ~68.5 Ma, and (d) ~62.5 Ma time. Explanations to the legend are as follows: (1) Major continental blocks, (2) microcontinents, (3) ultra-thinned continental crust, (4) volcanics, (5) rift axis, (6) ridge axis, (7) transform fault, (8) extinct spreading centre, (9) palaeo-transform fault, (10) the Gop-Narmada-Laxmi fossil triple junction off the Saurashtra peninsula. Red and pink coloured arrows represent the directions of spreading and rifting, respectively. The names of geographical domains or topographical features (after Bhattacharya and Chaubey, 2001 and Bhattacharya and Yatheesh, 2015) are abbreviated as follows: ABB, Arabian Basin; ATTC, Alleppey-Trivandrum Terrace Complex; ESB, Eastern Somali Basin; LAX, Laxmi Ridge continental sliver; LCP, Laccadive Plateau; LXB, Laxmi Basin; MDR, Madagascar Ridge; MSB, Mascarene Basin; SEY, Seychelles Plateau; SVP, Saurashtra Volcanic Platform. The northern boundary of the Indian subcontinent, with Greater India to its north, is shown by a dashed line. A now-submerged Mauritia continent has been postulated (Ashwal et al., 2017) between India and Madagascar. The northern part of the Chagos-Laccadive Ridge (i.e., the Laccadive Plateau), which has continental characteristics as suggested by a large number of multichannel deep-penetrating seismic reflection profiles and seismic refraction data, may be a part of Mauritia (Bhattacharya and Yatheesh, 2015). The four panels also show the correlatives of the Indo-Madagascar flood basalt province in southern India, along with the Antampombato (89.9 Ma), Ambohiby (90.0 Ma) and Maningoza (93.4) volcano-plutonic complexes in Madagascar (Melluso et al., 2005; Finkelstein, 2010; Mukosi, 2012), and the multiple magmatic phases now identified in the Sarnu-Dandali and Mundwara complexes of Rajasthan (Pande et al., 2017 and the present study). Note that Early Cretaceous basalt in the Sarnu-Dandali complex (panel *a*) is identified stratigraphically, and is too altered to be radio-isotopically dated (Bladon et al., 2015a).

Cucciniello et al., 2010, 2013, 2015; Mahoney et al., 1991; Melluso et al., 2003; Storetvedt et al., 1992; Storey et al., 1997), along with smaller volumes of rhyolitic rocks and mafic to felsic alkaline rocks (e.g., Kshirsagar et al., 2011; Melluso et al., 2005, 2009; Zellmer et al., 2012). The alkaline complexes of Mundwara and Sarnu-Dandali in Rajasthan, northwestern India (Fig. 2), are considered to be a part of the Deccan province (though they are 500–800 km from the main flood basalt outcrop) based on a few $^{40}Ar/^{39}Ar$ ages of 68.5–64 Ma, available for whole-rock samples, biotite and amphibole (Basu et al., 1993; Rathore et al., 1996a). However, Pande et al. (2017) have obtained new $^{40}Ar/^{39}Ar$ ages of 80–84 Ma on primary biotites in mafic cumulate rocks and 102–110 Ma on nepheline syenites of Mundwara. They interpret the combined $^{40}Ar/^{39}Ar$ age data as indicating a polychronous emplacement history of the Mundwara complex, from the Early Cretaceous to the Late Cretaceous-Palaeocene time (corresponding to Deccan volcanism).

The Sarnu-Dandali complex is considered to represent an early alkaline phase of the Deccan flood basalt volcanism based on a *single* $^{40}Ar/^{39}Ar$ age of 68.57 ± 0.08 Ma (2σ) available for biotite from an alkali pyroxenite (Basu et al., 1993). However, a basalt flow underlying the Early Cretaceous Sarnu Sandstone was recently reported (Bladon et al., 2015a). In this study, we present six new $^{40}Ar/^{39}Ar$ ages from the Sarnu-Dandali complex. We find two distinct age groups of 88.9–86.8 Ma (five samples) and 66.3 Ma, which we relate to Indo-Madagascar and Deccan flood basalt volcanism, respectively. The new $^{40}Ar/^{39}Ar$ ages show a polychronous emplacement of the Sarnu-Dandali complex, as shown for the Mundwara complex (Pande et al.,

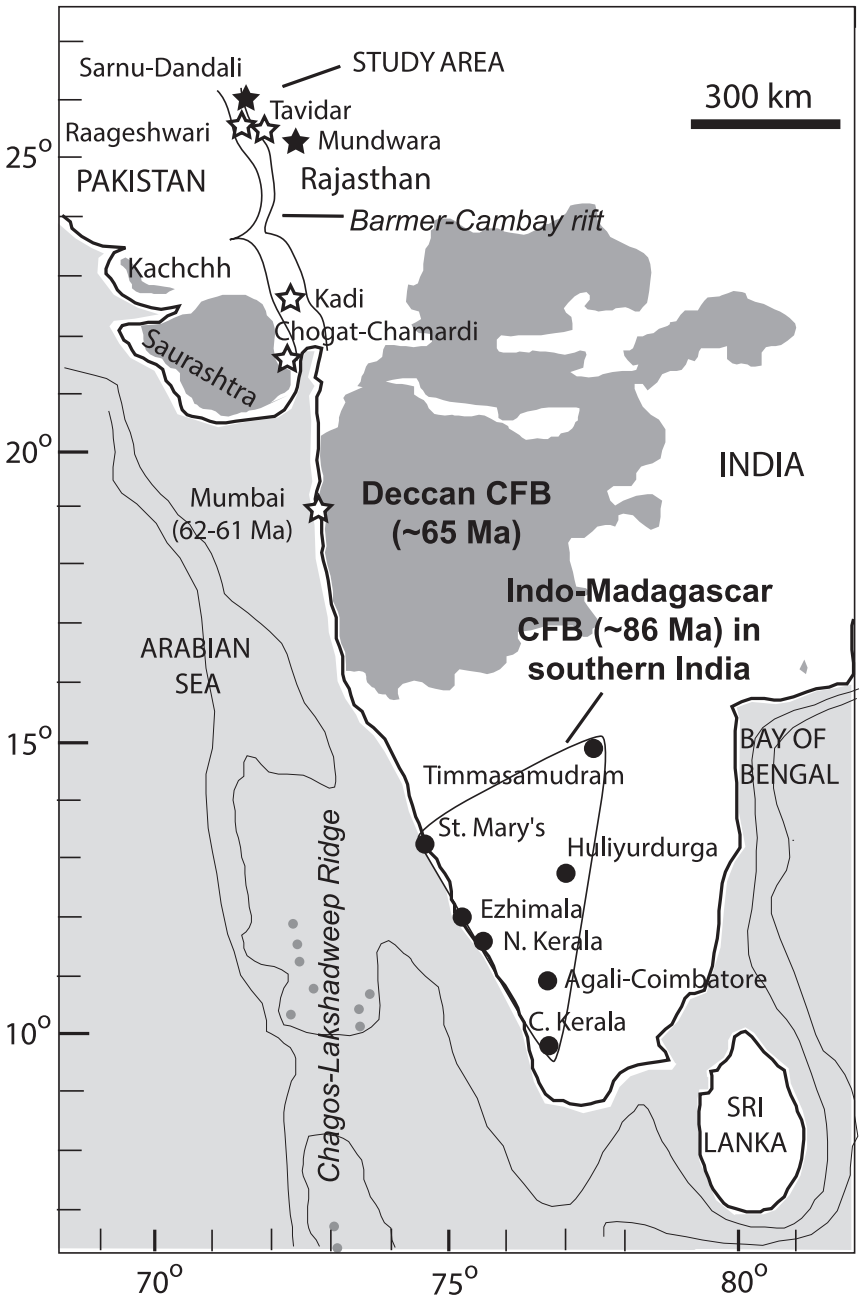

Fig. 2. Map of India and the Deccan Traps (modified from Vijayan et al., 2016) with some volcano-plutonic complexes in the northwestern Deccan region marked (black stars). SD is the Sarnu-Dandali complex, TV the Tavidar volcanics, RV the Raageshwari volcanics, MM the Mundwara (syn. Mer Mundwara) complex, K the Kadi syenite pluton, and CC the Chogat-Chamardi complex. Remnants of the Indo-Madagascar flood basalt province in southern India (Valsangkar et al., 1981; Torsvik et al., 2000; Pande et al., 2001; Kumar et al., 2001; Melluso et al., 2009; Radhakrishna and Joseph, 2012; Chalapathi Rao et al., 2016) are also shown.

2017). We discuss how the new results considerably improve our understanding of the Indo-Madagascar and Deccan flood basalt events and Late Cretaceous geodynamics in northwestern India.

2. Geology, rock types and samples, and whole-rock geochemistry

The Sarnu-Dandali complex is located on the eastern shoulder of the Barmer Basin, which initiated as a rift basin in the 750 Ma Malani rhyolite-granite basement during Early Cretaceous NW-SE extension. It underwent further major rifting during Late Cretaceous NE-SW extension, and contains >6 km thick Mesozoic (pre-rift Jurassic and within-rift Early to Late Cretaceous) sedimentary rocks with good hydrocarbon reserves (Bladon et al., 2015b; Dolson et al., 2015).

Bladon et al. (2015a) present stratigraphic relationships showing that a highly weathered basalt flow, hitherto undated, underlies the Early Cretaceous Sarnu Sandstone in the Sarnu Hills in the western part of the study area (Fig. 3; see this figure for all localities and sample locations). The Deccan-age Raageshwari volcanics (Bladon et al., 2015b) are present in the Barmer Basin at 3 km depth and the Deccan-age Tavidar volcanics on the eastern shoulder of the Barmer Basin (Fig. 2). The Barmer Basin and the Cambay Basin to its south (with igneous intrusions such as the Kadi syenite and the Chogat-Chamardi complex, Fig. 2) form a major, 600 km long, intracontinental rift ascribed to far-field stresses from ongoing Late Cretaceous plate reorganizations (Bladon et al., 2015b; see also Sharma, 2007).

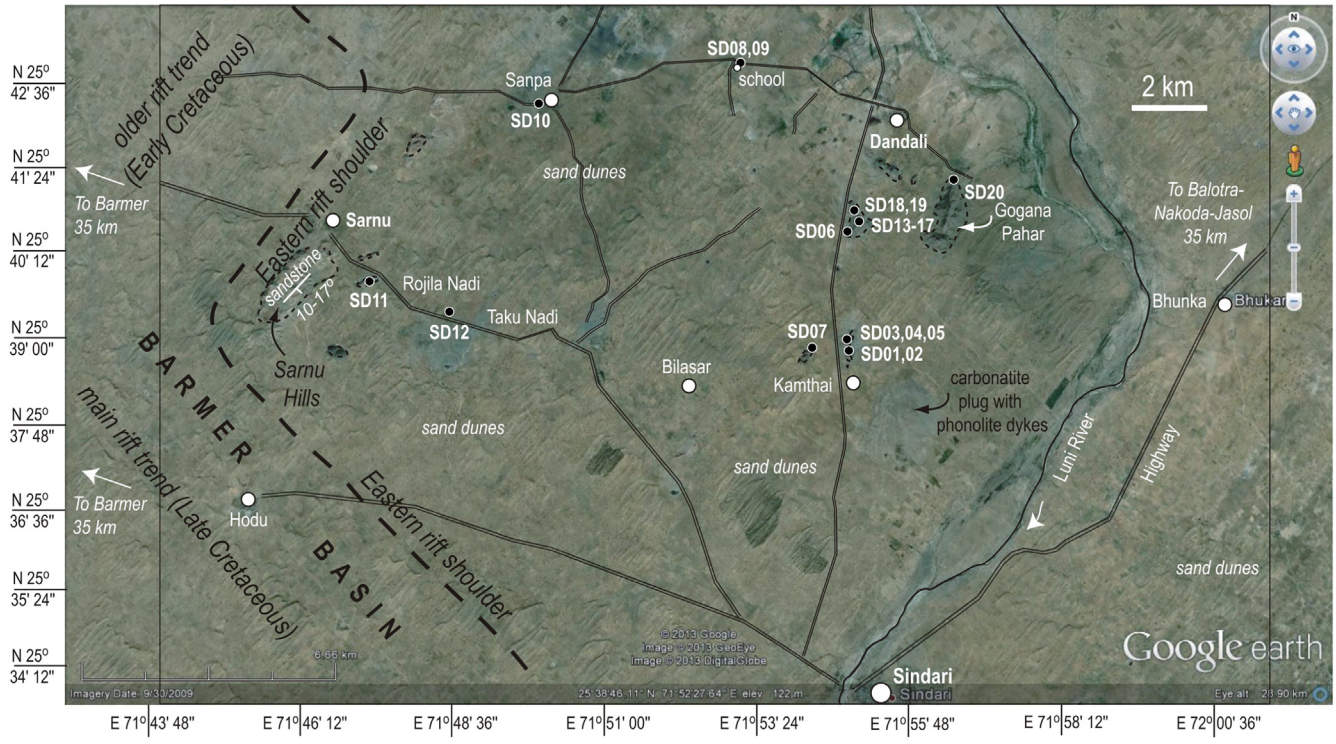

Fig. 3. Google Earth image of the study area of the Sarnu-Dandali complex, showing the largely sand dune-covered, flat landscape and the low hills, with villages, roads (thin double lines) and sample locations (with the prefix SD). Also marked is the eastern margin of the Barmer Basin (from Bladon et al., 2015a, 2015b). See Vijayan et al. (2016) for full geological descriptions.

The Sarnu-Dandali area (Fig. 3), ~100–140 m above sea level, is mostly flat with an extensive cover of Quaternary sands of the Rajasthan desert. The Malani rhyolites and the Early Cretaceous Sarnu Sandstone, with an underlying basalt flow, form the basement of the Sarnu-Dandali complex (Bladon et al., 2015a). The rocks of the complex form subvolcanic plutons, dykes as well as lava flows, and comprise mafic (nephelinites, melanephelinites, alkali pyroxenites) to felsic (alkali syenites, phonolites) alkaline rocks and carbonatites (e.g., Bhushan and Chandrasekaran, 2002; Srivastava, 1989; Vijayan et al., 2016; Viladkar, 2015). Geological field relationships as well as tectonic aspects of the complex have been described by Vijayan et al. (2016), who also present geochemical data (the major elements and loss on ignition values, several trace elements, and CIPW norms) for 19 samples, including the samples dated in this study (Table 1).

To determine the emplacement ages and duration of the complex, six rock samples (syenites SD13 and SD20, nephelinite SD14, phonolite SD19, rhyolite SD01, and melanephelinite SD11) were chosen for dating by the $^{40}Ar/^{39}Ar$ incremental heating technique. The samples are generally fresh with low to moderate loss on ignition (LOI) values. Sample SD13 represents a fresh coarse-grained (>1 cm) peralkaline syenite pluton exposed halfway between Kamthai and Dandali (Fig. 3). It contains numerous mafic enclaves (Fig. 4a), derived from synplutonic mafic injections in the largely molten syenite pluton. It is also intruded by many coherent dykes emplaced after pluton solidification, such as a nephelinite dyke striking N40°W (Fig. 4b; sample SD14) and a phonolite dyke striking N15°W (Fig. 4c; sample SD19). Sample SD20 was taken 2.5 km southeast of Dandali, at the northern end of another syenite pluton that forms the hill of Gogana Pahar (Fig. 4d). Sample SD01 comes from a black, moderately porphyritic rhyolite plug just north of Kamthai village. Plugs and dykes of phonolite and rhyolite are found here. Sample SD11 is a highly porphyritic melanephelinite lava flow outcropping 2 km southeast of Sarnu. It is subhorizontal, >20 m thick and shows colonnade and entablature tiers (Fig. 4e).

3. Petrography

Rock weathering produces alteration minerals, which are much less retentive of argon than the primary minerals, because of their open crystal structures. The mobility of both K and Ar during rock alteration may significantly affect the $^{40}Ar/^{39}Ar$ ages (e.g., Iwata and Kaneoka, 2000; McDougall and Harrison, 1999; Baksi, 2007, and many others). We carried out petrographic examination of the samples dated in this study as a qualitative means to assess their alteration state (besides the assessments based on LOI values). We also carried out a mineral chemical study of the rocks' primary mineral phases as a means of comparison to similar rock suites.

The modal (volumetric) proportions of minerals in the rocks were determined by point counting with Leica QwinPlus software image analysis (counting 1500 points in each thin section). The peralkaline syenite SD13 (LOI 0.74 wt.%) is coarse-grained with hypidiomorphic texture. Its mineral assemblage includes euhedral to subhedral alkali feldspar (84%) and amphibole (10%), rare mica (2%), apatite (~1%), Fe-Ti oxides (~1%), titanite (~1%) and zircon (~1%). In Fig. 5a, SD13 shows large intergrown crystals of perthitic alkali feldspar, along with several grains of biotite. Nephelinite SD14 (LOI 1.61 wt.%) is rich in clinopyroxene phenocrysts, some of which have a swallowtail shape. SD14 also has subhedral nepheline and perovskite phenocrysts, with nepheline, sodalite, mica, perovskite, and rare alkali feldspars forming the groundmass (Fig. 5b). Phonolite SD19 is considerably weathered with a LOI value of 4.56 wt.%. It has a few alkali feldspar and mica phenocrysts with aggregates of fine-grained clinopyroxene, and a fine-grained groundmass with a distinct flow texture defined by alkali feldspar microlites (Fig. 5c). Alkali feldspars, sodalite, analcime and clinopyroxene form the groundmass. Syenite SD20 (LOI 2.23 wt.%) shows a hypidiomorphic texture (Fig. 5d) and consists of perthitic alkali feldspar (85%), mica (5%), opaque oxides (5%), apatite (2%), quartz (~2%) and zircon (~1%). Rhyolite SD01 (LOI 1.71 wt.%) contains a few

Table 1
Geochemical data for the Sarnu-Dandali alkaline rocks dated in this study.

Nature	Plug	Flow	Pluton	Dyke	Dyke	Pluton
Sample	**SD1**	**SD11**	**SD13**	**SD14**	**SD19**	**SD20**
Rock type	Rhyolite	Melanephelinite	Peralkaline syenite	Nephelinite	Phonolite	Syenite
SiO_2	71.72	34.99	63.65	43.24	50.94	61.72
TiO_2	0.44	5.09	0.60	1.76	0.41	0.77
Al_2O_3	10.64	10.44	16.89	18.79	20.43	16.65
Fe_2O_{3T}	6.97	16.85	3.84	8.84	3.98	3.57
MnO	0.05	0.17	0.14	0.29	0.19	0.23
MgO	0.05	9.92	0.53	1.66	0.32	0.50
CaO	0.89	13.59	1.00	6.67	1.90	2.72
Na_2O	3.12	2.64	7.52	10.13	11.31	7.07
K_2O	4.82	2.09	4.85	4.47	4.70	4.55
P_2O_5	0.06	0.73	0.14	0.41	0.09	0.14
LOI	1.71	2.17	0.74	1.61	4.56	2.23
Total	100.47	98.68	99.88	97.86	98.84	100.15
Mg#	2.02	57.9	28.3	33.5	18.6	28.6
Q	32.05	–	–	–	–	–
Or	28.98	–	28.99	–	29.57	27.55
Ab	26.87	–	59.85	–	17.38	58.15
An	0.80	11.00	–	–	–	0.26
Lc	–	10.19	–	21.67	–	–
Ne	–	12.72	0.39	40.67	36.05	1.68
Ac	–	–	3.33	7.08	3.80	–
Di	2.95	15.60	3.51	19.38	8.15	8.88
Hy	4.17	–	–	–	–	–
Ol	-	23.58	2.39	2.42	0.83	–
Mt	3.19	3.92	0.08	–	–	1.64
Il	0.86	10.17	1.14	3.50	0.83	1.49
Ap	0.13	1.78	0.32	0.99	0.23	0.34
Ns	–	–	–	1.52	3.15	–
Cs	–	11.04	–	2.76	–	–
Sc	0.38	37.8	1.88	1.54	bdl	1.92
Co	3.90	74.0	4.27	18.7	2.23	4.91
Ni	40.0	108	8.25	4.55	3.81	8.77
Sr	28.5	930	180	2252	983	176
Zr	1165	282	606	426	669	152
Ba	72.5	835	800	1203	1283	1586

Notes: Major oxides and CIPW norms (italics) are in wt.%, and the trace elements are in parts per million (ppm). The norms were computed by the SINCLAS program of Verma et al. (2002), based on LOI-free recalculated data and the Middlemost (1989) scheme of division of total iron into Fe^{2+} and Fe^{3+} categories. *Ns* is sodium metasilicate and *Cs* calcium silicate. Rock types (names) are also as determined by SINCLAS based on the total alkali-silica diagram. Fe_2O_{3T} is total iron expressed as Fe_2O_3. "bdl" indicates concentration below detection limit. The data are from Vijayan et al. (2016); please see that paper for data for the whole sample suite, and information about analytical procedures and accuracy.

phenocrysts of altered perthitic K-feldspar and quartz, with a fine-grained groundmass made up of alkali feldspars, quartz, and Fe-Ti oxides (Fig. 5e). Melanephelinite SD11 (LOI 2.17 wt.%) is rich in clinopyroxene phenocrysts, which sometimes have marginal zones of a different composition, and nepheline is present in the groundmass (Fig. 5f).

4. Mineral chemistry

4.1. Analytical techniques

Mineral compositions were determined at the Instituto di Geologia Ambientale e Geoingegneria (CNR, Rome, Italy) using a Cameca SX50 electron microprobe that was equipped with five wavelength-dispersive spectrometers (WDS). The operating conditions were as follows: accelerating voltage 15 kV, beam current 15 nA, beam diameter 1 μm for olivine, pyroxene, and oxides, and 5 μm for feldspars, amphiboles, micas, etc. Na and K were analysed first to avoid alkali volatilization. Counting time was 20 s per peak element and 10 s for background (low and high). The following standards were used: wollastonite (Si and Ca), corundum (Al), periclase (Mg), magnetite (Fe), rutile (Ti), orthoclase (K), jadeite (Na), phlogopite (F), KCl (Cl), baritina (S and Ba), and metals (Cr, Mn). In order to evaluate the accuracy of the analyses, three international secondary standards (Kakanui augite, Icelandic basalt BIR-1 and rhyolite RLS132 glasses from the U.S. Geological Survey) were measured prior to any series of measurements. The mean precision was about 1% for SiO_2, 2% for Al_2O_3, 5% for K_2O, CaO and FeO, and 8–9% for the other elements. Matrix correction calculations were performed using the PAP procedure after Pouchou and Pichoir (1984).

4.2. Mineral compositions

4.2.1. Feldspars

Plagioclase is absent among the Sarnu-Dandali rocks studied here. Alkali feldspar is present in all rocks. It is the main mineral in the syenites SD13 and SD20, phonolite SD14 and rhyolite SD01. It is an extremely rare groundmass phase in the nephelinite SD14. Its composition is potassic ($An_0Ab_{5-13}Or_{95-87}$). In the rhyolite SD01, alkali feldspar ranges from anorthoclase ($An_0Ab_{83}Or_{17}$) to potassic sanidine ($An_0Ab_3Or_{97}$). Alkali feldspar in the syenites is mostly anorhoclase ($An_{0-6}Ab_{63-75}Or_{37-20}$) (Fig. 6a; Table S1). Feldspar in the phonolite SD19 is sanidine ($An_{0-1}Ab_{5-10}Or_{90-95}$) and has up to 3.3 wt.% of BaO. Ba-rich sanidine (up to 7.4 wt.% BaO) has been observed in the melaphonolites of Barmer, near Sarnu-Dandali (Viladkar, 2015).

4.2.2. Feldspathoids

Nepheline and sodalite (less abundant) constitute the feldspathoids in nephelinite SD14. Nepheline is silica-poor ($Ne_{73-74}Ks_{24-25}Qz_2$). CaO ranges from 0.1 to 1.6 wt.% (Table S2). Nepheline is commonly replaced by analcime in the phonolite SD19. Sodalite occurs as a groundmass phase in the nephelinite SD14 and phonolite SD19. It is low in K (up to 0.4 wt.% K_2O) and Ca (up to 1.2 wt.% CaO; Table S2).

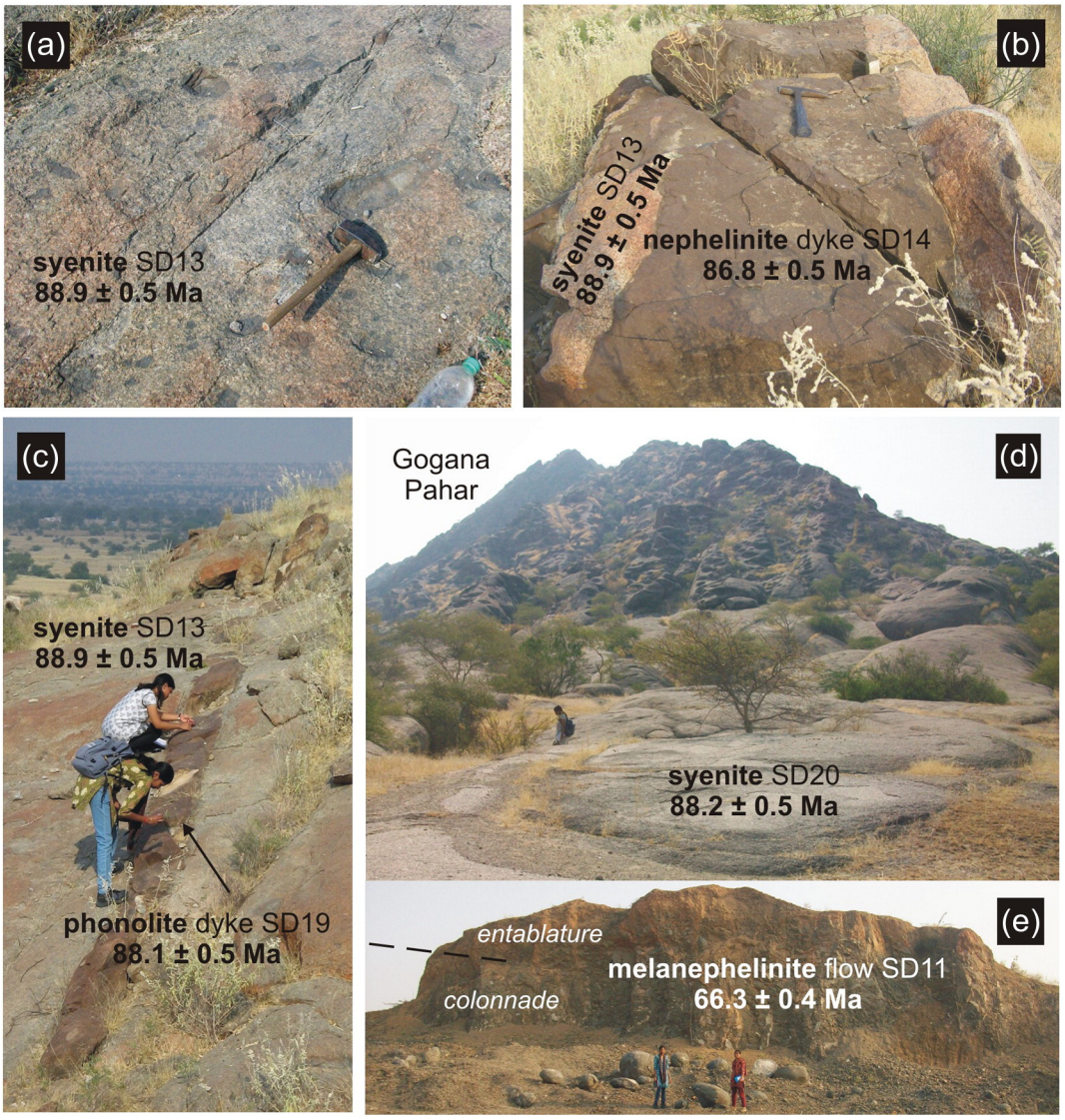

Fig. 4. Geological relationships between rock units dated, with ages and 2σ uncertainties. (a) Peralkaline syenite pluton SD13 with mafic enclaves. (b) Nephelinite dyke SD14 intruding syenite SD13. Dyke is up to 2 m wide and strikes N40°W. (c) Phonolite dyke SD19 intruding syenite SD13. Dyke is up to 0.45 m wide and strikes N15°W. (d) Syenite SD20 sampled in low ground north of Gogana Pahar hill. Person for scale. (e) Melanephelinite lava flow SD11 near Sarnu. The colonnade and entablature tiers of the flow are shown, along with their relatively sharp boundary (dashed black line). Students provide a scale.

4.2.3. Clinopyroxene

Clinopyroxene of nephelinite SD14 is diopside and plots mostly above the diopside-hedenbergite join in the Ca-Mg-Fe diagram (Fig. 6b) suggesting significant amounts (up to 21 mol%) of non-tetrahedral, low-pressure end-members such as $CaTiAl_2O_6$ and $CaFe^{3+}AlSiO_6$. The clinopyroxene Mg# values range from 68 to 76, with maximum TiO_2 and Al_2O_3 contents of 3.0 and 5.5 wt.%, respectively. Clinopyroxene of phonolite SD19 is aegirine (Na_2O = 12.9 wt.%). This type of clinopyroxene typically crystallizes from melts that reached peralkaline compositions The Al_2O_3 and TiO_2 contents are low (Table S3).

4.2.4. Amphibole

Amphibole occurs only in the syenite SD13. It is an edenite (according to the IMA 1997 nomenclature rules, Leake et al., 1997) and shows a moderate range in Mg# (52–62) and TiO_2 content (0.19–1.66 wt.%). Na_2O (3.35–3.95 wt.%) and K_2O (0.71–1.02 wt.%) are roughly constant. F ranges from 1.54 to 1.69 wt.% suggesting a relatively high fluorine activity. Amphibole analyses are reported in Table S4 and Fig. 6c.

4.2.5. Mica

Mica in the syenites occurs as interstitial phase or as inclusions in other minerals. It has Mg# = 60–71, Al_2O_3 = 11.6–12.4 wt.% and TiO_2 = 3.0–4.4 wt.%. Phenocrysts of mica in the phonolite SD19 have lower Mg# (42–61) than micas of the syenites. TiO_2 and Al_2O_3 range from 2.9 to 5.0 wt.% and from 10.6 to 13.2 wt.%, respectively. Mica of the nephelinite SD14 is TiO_2-poor (0.58 wt.%) and has Mg# = 69 (Fig. 6d; Table S5).

4.2.6. Magnetite and ilmenite

Magnetite in the Sarnu-Dandali rhyolite SD01 and the syenites SD13 and SD14 is poor in Ti (from 3 to 23 mol% ulvöspinel) (Table S6). Ilmenite ($ilm_{95–97}$) has been found only in the syenites. The compositions are low in Al (<0.02 wt.% Al_2O_3). Equilibration temperatures for syenites based on the magnetite-ilmenite geothermometer (Lepage, 2003) range between 588 and 607 °C. These values indicate re-equilibration under subsolidus conditions. The oxygen fugacity ranges from −19.5 to −21.1 log units.

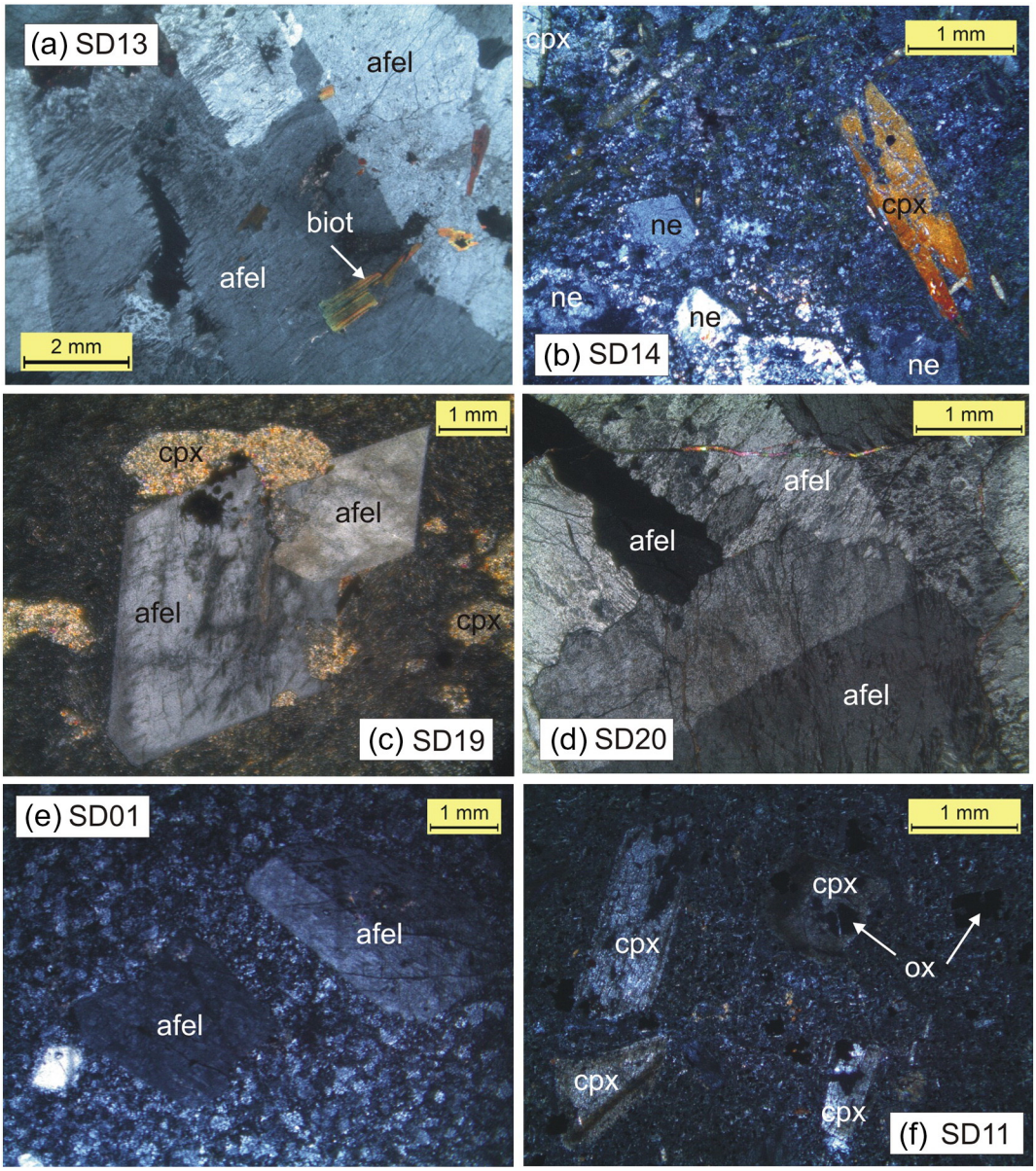

Fig. 5. Photomicrographs of the dated samples, all taken between crossed nicols. (a) Peralkaline syenite SD13. (b) Nephelinite SD14. (c) Phonolite SD19. (d) Syenite SD20. (e) Rhyolite SD01. (f) Melanephelinite SD11.

4.2.7. Perovskite, apatite, titanite and zircon

Perovskite has been found as microphenocryst and groundmass phase in the nephelinite SD14. It shows a composition close to the pure $CaTiO_3$ component (Table S7). Apatite typically occurs as microlites in the groundmass of nephelinite SD14 or as inclusions in other minerals in the syenites. It has high F content (3.6–4.9 wt.%). SrO ranges from 0 to 1.4 wt.% (Table S7). Titanite occurs as euhedral to subhedral crystals in the syenite SD13. It has a homogeneous major element composition (Table S7). Zircon is ubiquitous as small grains in the syenites (Table S7).

5. $^{40}Ar/^{39}Ar$ geochronology

5.1. Analytical techniques

Rock chips of about 20–25 g were cut from the hand specimens to avoid veins and weathered material, then crushed and sieved, and cleaned in deionized water in an ultrasonic bath. About 0.02 g of each was packed in aluminium capsules. The Minnesota hornblende reference material (MMhb-1) of age 523.1 ± 2.6 Ma (Renne et al., 1998) and high-purity CaF_2 and K_2SO_4 salts were used as monitor samples. High-purity nickel wires were placed in both sample and monitor capsules to monitor the neutron fluence variation, which was typically ~5%. The aluminium capsules were kept in a 0.5 mm thick cadmium cylinder and irradiated in the heavy water-moderated DHRUVA reactor at the Bhabha Atomic Research Centre (BARC), Mumbai, for ~100 h. The irradiated samples were repacked in aluminium foil and loaded on the extraction unit of a Thermo Fisher Scientific noble gas preparation system. Argon was extracted in a series of steps up to 1400 °C in an electrically heated ultrahigh vacuum furnace. After purification using Ti-Zr getters, the argon released in each step was measured with a Thermo Fisher ARGUS VI mass spectrometer located at the National Facility for $^{40}Ar/^{39}Ar$ Geo-thermochronology in the Department of Earth Sciences, IIT Bombay. The mass spectrometer is equipped with five Faraday cups fitted with 10^{11} Ω resistors.

Interference corrections for Ca- and K-produced Ar isotopes based on analysis of CaF_2 and K_2SO_4 salts were $(^{36}Ar/^{37}Ar)_{Ca}$, $(^{39}Ar/^{37}Ar)_{Ca}$ and $(^{40}Ar/^{39}Ar)_K = 0.000491$, 0.001277 and 0.013001, respectively.

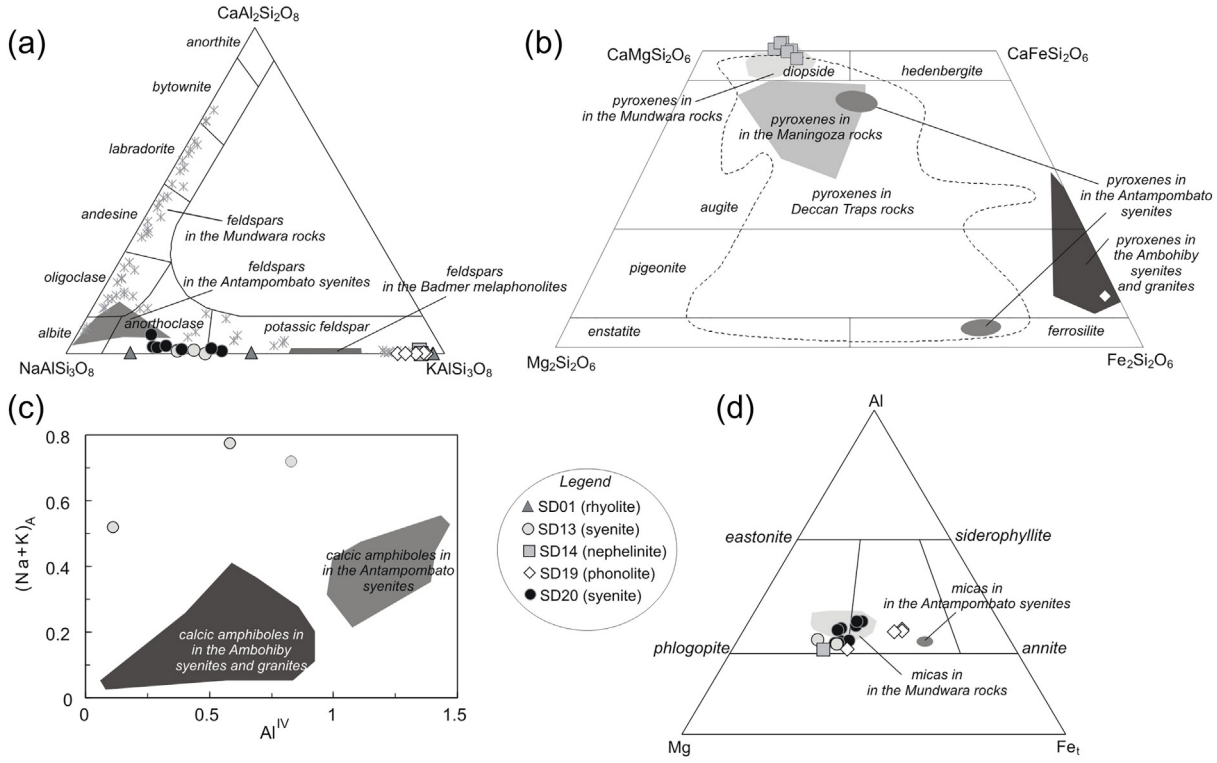

Fig. 6. Mineral compositions in the 88.9–86.8 Ma Sarnu-Dandali rocks. (a) Feldspar compositions. Chemical compositions of feldspars from the Mundwara complex (Pande et al., 2017), Barmer melaphonolites (Viladkar, 2015) and the Antampombato syenites (Melluso et al., 2005) are also shown. (b) Pyroxene compositions from the nephelinite SD14 and phonolite SD19 projected in the Ca-Mg-Fe diagram. Compositional fields are shown for pyroxenes of the Mundwara complex (Pande et al., 2017), the Deccan Traps including the Saurashtra region of the northwestern Deccan (Melluso and Sethna, 2011 and references therein; Cucciniello et al., 2015 and references therein, L. Melluso, unpubl. data), and the Antampombato and Ambohiby syenites (Melluso et al., 2005; Mukosi, 2012). (c) $(Na + K)_A$ vs. Al^{IV} cation diagram for the Sarnu-Dandali calcic amphiboles. Chemical compositions of calcic amphiboles from the Antampombato and Ambohiby syenites (Melluso et al., 2005; Mukosi, 2012) are also shown. (d) Al-Mg-Fe ternary diagram for the Sarnu-Dandali micas. Mica compositions of Mundwara rocks (Pande et al., 2017) and the Antampombato syenites (Melluso et al., 2005) are also shown.

^{40}Ar blank contributions were 1–2% or less for all temperature steps. Values of the irradiation parameter *J* for each sample, after correction for neutron flux variation, are as follows: SD13 (0.0006284 ± 0.0000033), SD14 (0.0006834 ± 0.0000035), SD19 (0.0006790 ± 0.0000035), SD20 (0.0006776 ± 0.0000034), SD01 (0.0006884 ± 0.0000033), SD11 (0.0006794 ± 0.0000035). The plateau ages reported comprise a minimum of 50% of the total ^{39}Ar released and four or more successive degassing steps whose mean ages overlap at the 2σ level excluding the error contribution (0.5%) from the *J* value. The data were plotted using the program Isoplot/Ex v. 3.75 (Ludwig, 2012).

5.2. Results

Table 2 gives the summary of the ^{40}Ar/^{39}Ar results (plateau, isochron and inverse isochron ages with 2σ uncertainties) for the six Sarnu-Dandali rock samples. Plateau spectra and isochron plots for the six samples are shown in Figs. 7 and 8. The stepwise analytical data are given in Table S8.

The peralkaline syenite pluton SD13 yielded a good 7-step plateau constituting 54.5% of the ^{39}Ar release and an age of 88.9 ± 0.5 Ma (2σ) (Fig. 7a). The lower-temperature gas fractions that constitute the

Table 2
Summary of ^{40}Ar/^{39}Ar dating results for the Sarnu-Dandali alkaline complex, Rajasthan.

Sample	Plateau					Isochron				Inverse isochron			
	Steps	%^{39}Ar	Age (Ma)	MSWD	*p*	Age (Ma)	Trap	MSWD	*p*	Age (Ma)	Trap	MSWD	*p*
SD13 Peralk.syenite	7	54.6	88.9 ± 0.5	0.11	1.00	88.9 ± 0.7	296.2 ± 3.3	0.11	0.99	88.9 ± 0.6	295.9 ± 2.4	0.15	0.98
SD14 Nephelinite	8	52.9	86.8 ± 0.5	0.11	1.00	86.8 ± 2.3	296 ± 130	0.02	1.00	86.7 ± 1.2	300 ± 60	0.10	1.00
SD19 Phonolite	9	42.1*	88.1 ± 0.5	0.11	1.00	88.1 ± 0.6	295.9 ± 3.1	0.03	1.00	88.1 ± 0.5	295.7 ± 2.3	0.10	1.00
SD20 Syenite	5	30.7*	88.2 ± 0.5	0.22	0.93	87.9 ± 2.9	298 ± 26	0.14	0.94	87.9 ± 2.0	299 ± 18	0.27	0.85
SD01 Rhyolite	7	56.0	87.3 ± 0.5	0.16	0.99	87.1 ± 1.6	311 ± 91	0.01	1.00	87.2 ± 0.7	308 ± 35	0.05	1.00
SD11 Mela-nephelinite	8	49.5	66.3 ± 0.4	0.24	0.98	66.3 ± 1.7	291 ± 83	0.05	1.00	66.3 ± 0.8	295 ± 33	0.19	0.98

Notes: * indicates that the plateau spectra for these samples contain ≪50% of the total ^{39}Ar released and therefore do not fully satisfy the criteria for a plateau age adopted in this paper (see text). Trap is initial ^{40}Ar/^{36}Ar ratio (trapped component), MSWD is Mean Square Weighted Deviate and *p* is the corresponding probability. Errors are reported at the 2σ confidence level and monitor mineral is MMhb-1 (523.1 ± 2.6 Ma, Renne et al., 1998). Decay constants used are those of Steiger and Jager (1977). All samples are whole-rock samples. GPS locations of the samples are as follows: SD13 (25°40′47″ N, 71°54′54″ E), SD14 (25°40′47″ N, 71°54′54″ E), SD19 (25°40′49″ N, 71°54′52″ E), SD20 (25°41′20″ N, 71°56′32″ E), SD01 (25°38′53″ N, 71°54′34″ E), SD11 (25°39′51″ N, 71°47′19″ E).

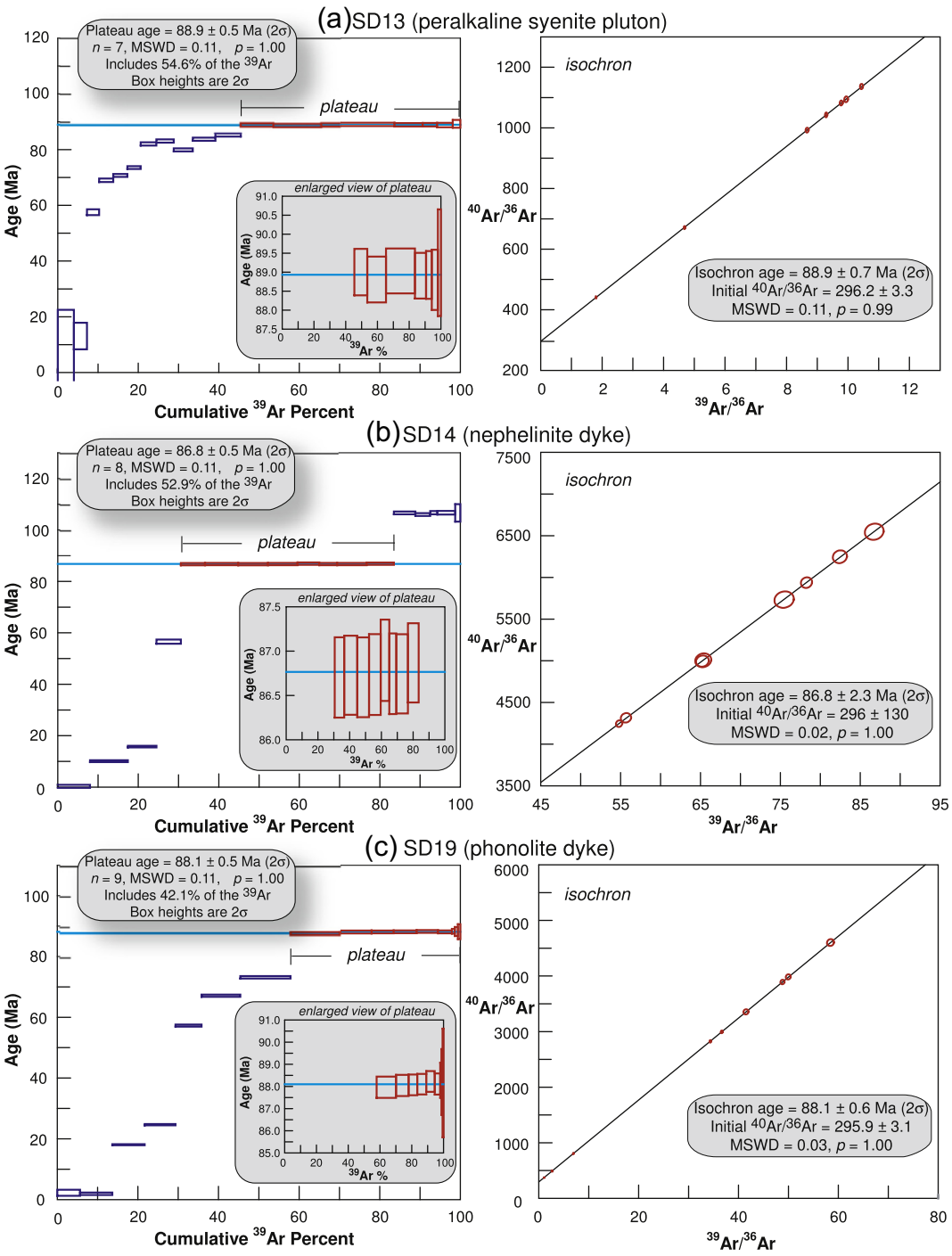

Fig. 7. $^{40}Ar/^{39}Ar$ plateau spectra and isochrons for (a) peralkaline syenite pluton SD13, (b) nephelinite dyke SD14, and (c) phonolite dyke SD19. The plateau steps are shown with brackets. Also shown are values of the MSWD (mean square weighted deviate) and probability (p). Along with each complete plateau spectrum, enlarged views of just the plateau part of the spectrum are also provided.

non-plateau part of the spectrum define an ascending staircase pattern. Nephelinite dyke SD14 also yielded a good 8-step plateau constituting 52.9% of the ^{39}Ar release and an age of 86.8 ± 0.5 Ma (2σ) (Fig. 7b). Phonolite dyke SD19 yielded a 9-step plateau constituting 42.1% of the ^{39}Ar release and an age of 88.1 ± 0.5 Ma (2σ) (Fig. 7c). The non-plateau part of the spectrum shows an ascending staircase pattern. The plateau spectrum for SD19 does not strictly meet our criterion of minimum 50% of ^{39}Ar release, and so is a marginal plateau. Sample SD19 is altered with a high LOI of 4.56 wt.%. Nevertheless, all three samples have isochron ages and inverse isochron ages, which are statistically indistinguishable from the plateau ages (Fig. 7a-c and Table 2). The isochrons and inverse isochrons also have acceptable MSWD values and intercepts showing atmospheric $^{40}Ar/^{36}Ar$ ratios of the trapped argon (295.5), suggesting that they are crystallization ages. The ages are also fully consistent with the geological field relationships. Dykes SD14 and SD19 are both intrusive into the syenite pluton SD13, and the ages and their uncertainties indicate that SD14 is significantly younger than SD13 (a minimum of 0.9 and a maximum of 3.3 million years). SD19 could be coeval with, or up to 1.8 million years younger than syenite SD13.

The Gogana Pahar syenite pluton SD20 yielded a spectrum with a wide range of ages for the individual steps, and a 5-step marginal plateau with 30.7% of the ^{39}Ar release and an age of 88.2 ± 0.5 Ma

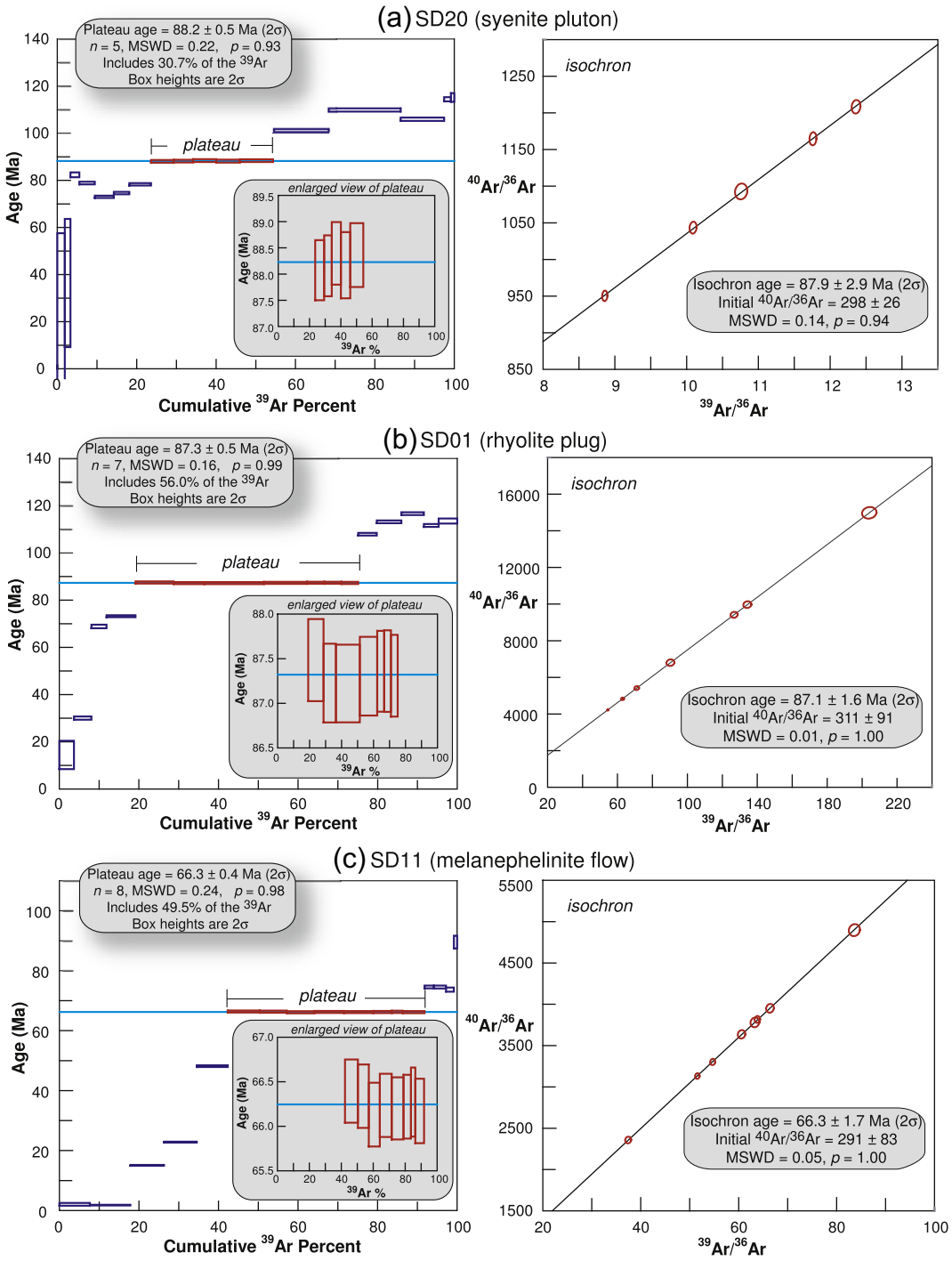

Fig. 8. $^{40}Ar/^{39}Ar$ plateau spectra and isochrons for (a) syenite pluton SD20, (b) rhyolite plug SD01, and (c) melanephelinite lava flow SD11.

(2σ) (Fig. 8a). This may also be due to alteration (LOI is 2.23 wt.%). The rhyolite plug SD01 near Kamthai yielded a good 7-step plateau comprising 56.0% of the ^{39}Ar release and an age of 87.3 ± 0.5 Ma (2σ) (Fig. 8b). Melanephelinite lava flow SD11 near Sarnu yielded an 8-step plateau comprising 49.5% of the ^{39}Ar release and an age of 66.3 ± 0.4 Ma (2σ) (Fig. 8c). Again, the isochrons and inverse isochrons have acceptable MSWD values and atmospheric $^{40}Ar/^{36}Ar$ ratios (295.5) of the trapped argon, and yield ages statistically indistinguishable from the plateau ages (Fig. 8a-c and Table 2), implying that they represent the time of crystallization.

The striking observation based on these data is that five of the six samples are 88.9–86.8 Ma in age, and thus some 20 million years older than Deccan volcanism, whereas the 66.3 Ma age of the sixth sample (melanephelinite flow SD11) corresponds exactly to Deccan volcanism. Melanephelinites are common in the Deccan alkaline plugs of Kachchh, northwestern India (Fig. 1; Kshirsagar et al., 2011).

6. Discussion

6.1. Regional implications of the $^{40}Ar/^{39}Ar$ results

Basu et al. (1993) and Rathore et al. (1996a) provided $^{40}Ar/^{39}Ar$ ages of ~68.5–64 Ma on mineral separates (primary biotite and amphibole) and whole-rock samples from the Mundwara alkaline complex. The

Mundwara complex, 120 km southeast of Sarnu-Dandali, lies outside the Barmer Basin on 1100–850 Ma Erinpura Granite basement (Fig. 2). Radioisotopic dating of the Sarnu-Dandali complex is limited to a single $^{40}Ar/^{39}Ar$ age of 68.57 ± 0.08 Ma (2σ) for biotite from an alkali pyroxenite (Basu et al., 1993). Based on these ages, the Mundwara and Sarnu-Dandali complexes have been considered to be distant outliers of the ~65 Ma (Late Cretaceous to Palaeocene) Deccan Traps flood basalt province (Fig. 2), and as representing Deccan alkaline magmatism which immediately preceded the massive flood basalt phase (Basu et al., 1993). Both complexes have also been equated (Devey and Stephens, 1992; Ganerød et al., 2011) to Deccan-age alkaline complexes in the Seychelles, which was joined to northwestern India until ~62 Ma (Collier et al., 2008; Ganerød et al., 2011).

However, the new $^{40}Ar/^{39}Ar$ ages of Pande et al. (2017) on the Mundwara complex (80–84 Ma on biotite separates and 102–110 Ma on nepheline syenite whole-rocks) indicate a polychronous emplacement history. Some of the constituent Mundwara intrusions are of Deccan age but others are older and unrelated to the Deccan Traps, with the 110 Ma ones broadly contemporaneous with the Rajmahal Traps of eastern India (Kent et al., 2002). In the same manner, a polychronous emplacement history for the Sarnu-Dandali complex is indicated by the Early Cretaceous basalt flow in the Sarnu Hills (Bladon et al., 2015a) and our new $^{40}Ar/^{39}Ar$ age data. The $^{40}Ar/^{39}Ar$ ages indicate that the constituent rocks of this complex were emplaced during two distinct episodes during Late Cretaceous time. The 66.3 Ma age of the Sarnu melanephelinite flow (sample SD11) unambiguously corresponds to Deccan volcanism, but the 88.9–86.8 Ma ages on five samples (representing two syenite plutons, a nephelinite dyke and a phonolite dyke, and a rhyolite plug) show that the Sarnu-Dandali complex is dominantly a significantly older alkaline complex than the Deccan Traps.

Our $^{40}Ar/^{39}Ar$ dating results have additional implications for magmatic evolution and tectonics. The 87.3 ± 0.5 Ma (2σ) age for the rhyolite plug near Kamthai (sample SD01) shows that not all rhyolites exposed around Sarnu-Dandali are 750 Ma Malani rhyolites. A N20°W-striking peralkaline rhyolite dyke that cuts this pluton (sample SD03 of Vijayan et al., 2016) is contemporaneous or younger. Rhyolite magma is thus an integral part of the Sarnu-Dandali petrogenetic lineage. Vijayan et al. (2016) noted that >95% of the dykes in the Sarnu-Dandali complex trend NNW-SSE. They argued that this reflected a contemporaneous regional stress field (with a ENE-WSW σ_3) rather than control by basement structural fabric. The new $^{40}Ar/^{39}Ar$ results mean that their tectonic interpretations should relate to the 88.9–86.8 Ma time rather than the time of Deccan volcanism as perceived by them, but the fact that the extensional fractures and faults with the same trends are also found in overlying, Palaeocene-age rift sediments (Bladon et al., 2015b) may imply the continuity of the same stress field over ≥30 million years.

6.2. Broader implications for the Indo-Madagascar flood basalt province

An important observation is that our new $^{40}Ar/^{39}Ar$ ages of 88.9–86.8 Ma on five Sarnu-Dandali samples fall exactly within the time-frame of Indo-Madagascar flood basalt volcanism (~93–84 Ma) associated with the breakup of India and Madagascar. Remnants of this flood basalt volcanism are already known in southern India (Figs. 1, 2), whereas alkaline complexes broadly comparable to Sarnu-Dandali and Mundwara are known in Madagascar (Fig. 1). We therefore consider the 88.9–86.8 Ma Sarnu-Dandali complex as an integral part of the Indo-Madagascar flood basalt province. The counterparts of all these rock suites in the Mundwara complex, arguably corresponding to the post-breakup stage of the same flood basalt volcanism, are the 84–80 Ma biotite-bearing mafic plutonic rocks dated by Pande et al. (2017).

With the Sarnu-Dandali alkaline complex as a part of the Indo-Madagascar flood basalt province, the two Sarnu-Dandali rhyolites near Kamthai (SD01, SD03) are comparable to the St. Mary's Islands rhyolites on the southern Indian coast (Fig. 2), their geochemical correlatives around Vatomandry-Ilaka-Mananjary on the eastern Madagascar coast (Melluso et al., 2009), and the granophyre-dominated Ezhimala complex south of the St. Mary's Islands (Fig. 2) (Ram Mohan et al., 2016).

Late Cretaceous volcano-plutonic complexes in Madagascar (Fig. 1), broadly comparable to the Mundwara and Sarnu-Dandali complexes, include the 89.9 Ma Antampombato complex in central-eastern Madagascar, which contains dunites, wehrlites, clinopyroxenites, gabbros, and sodic syenites (Melluso et al., 2005). The 93.4 Ma Maningoza complex, in central-western Madagascar, is dominated by gabbros, basalts, rhyolites, syenites and granites (Finkelstein, 2010). The 90.0 Ma Ambohiby complex, in central Madagascar, contains gabbros, monzonites, alkali syenites, microgranites and granites (Mukosi, 2012). These volcano-plutonic complexes have strongly different magma types so that the search for a single source or liquid line of descent is almost meaningless. Nevertheless, we can provide some broad comparisons based on the mineral chemistry data acquired in this study. Amphiboles of edenitic composition occur in syenites from Sarnu-Dandali, Antampombato and Ambohiby complexes, but their differing minor element contents prevent any chemical correlation (Fig. 6c). In addition, the differences in the pyroxene (and other mineral) compositions rule out a common genesis of the Antampombato, Maningoza and Ambohiby complexes in Madagascar and the Sarnu-Dandali and Mundwara complexes in northwestern India.

The new 88.9–86.8 Ma $^{40}Ar/^{39}Ar$ ages for the Sarnu-Dandali rocks suggest that lithospheric extension related to the India-Madagascar breakup event and associated flood basalt volcanism was present in northwestern India hundreds of kilometres inwards of the rifting margins, as it was in the southern Indian examples (Fig. 2). The Sarnu-Dandali and Mundwara complexes, both showing Indo-Madagascar-age alkaline magmatism, are located 2000 km NNW of the southern Indian magmatic rocks related to the same event (see Fig. 2). We believe that additional outcrops of correlative rocks probably occur in between these two faraway groups of rocks, buried under the vast Deccan Traps (Figs. 1, 2). The combined areal extent of the Indo-Madagascar flood basalts (covering originally much of Madagascar, the oceanic Madagascar Plateau and Conrad Rise to its south, a 2000 km stretch of southern to northwestern India, and the possibly correlative seaward-dipping basalt reflectors identified on the western side of the Chagos-Lakshadweep Ridge (Ajay et al., 2010; see also Yatheesh et al., 2006) is thus really vast.

6.3. Broader implications for recurrent continental alkaline magmatism

Our results, like those of Pande et al. (2017), considerably improve our understanding of the Mesozoic magmatic history and crustal evolution in northwestern India. The combined age data now available for the Mundwara and Sarnu-Dandali alkaline complexes (Basu et al., 1993; Rathore et al., 1996a; Pande et al., 2017, and the present study) also show a remarkable parallel evolution for both complexes, with Early Cretaceous magmatism followed by two distinct magmatic episodes in the Late Cretaceous. The combined $^{40}Ar/^{39}Ar$ age data also establish these complexes as equivalent to many continental alkaline igneous centres around the world that show recurrent magmatism, sometimes over hundreds of millions of years. Barker (1974) provides examples from North America, and Bailey (1992) provides examples from Africa. An excellent example, particularly relevant in the present context, is the Silhouette-North Island complex in the Seychelles, where U/Pb zircon and $^{40}Ar/^{39}Ar$ dating have revealed distinct magmatic episodes in the Callovian (Mid-Jurassic, 163.8 Ma), Tithonian (Late Jurassic, 147.7 Ma), and Danian (Early Palaeocene, 64.9 Ma) (Ganerød et al., 2011; Shellnutt et al., 2015, 2017).

It is noteworthy that centres of repetitive alkaline magmatism on the African continent occur in regions affected by the Pan-African orogeny (Bailey, 1992; Bailey and Woolley, 2005). As argued by these workers, the deeper parts of orogenic belts, along which oceans have closed by continent-arc collisions, contain fertile, metasomatized mantle, which

can readily produce alkaline magmas during much later extensional tectonics. We note here that the thermal effects of the Pan-African orogeny in Rajasthan are now well-recognized, reflected in radiogenic argon loss events at ~500 Ma recorded from the Neoproterozoic Malani and Mount Abu granites and associated volcanics (Rathore et al., 1996b, 1999; Ashwal et al., 2013; Sen et al., 2013). We therefore relate the recurrent alkaline magmatism at Sarnu-Dandali and Mundwara to decompression melting of ancient, subduction-fluxed, enriched mantle lithosphere due to periodic lithospheric extension, from the Early Cretaceous through the Late Cretaceous and the Palaeocene, and hundreds of kilometres inland from the eventual India-Madagascar and India-Seychelles rifted margins.

7. Conclusions

New $^{40}Ar/^{39}Ar$ ages on the Sarnu-Dandali alkaline complex in Rajasthan, northwestern India, show that the constituent rocks of the complex were emplaced during two distinct periods, separated by 20 million years, in the Late Cretaceous. $^{40}Ar/^{39}Ar$ ages of 88.9–86.8 Ma on five samples (from syenite, nephelinite, phonolite and rhyolite subvolcanic intrusions) fully overlap with those for the Indo-Madagascar flood basalt province formed during continental breakup between India (plus Seychelles) and Madagascar. This event is also known from the polychronous Mundwara alkaline complex in Rajasthan, 100 km from Sarnu-Dandali (Pande et al., 2017). The $^{40}Ar/^{39}Ar$ age of 66.3 ± 0.4 Ma (2σ) obtained for a Sarnu-Dandali melanephelinite lava flow (this study), and a previously available age of 68.57 ± 0.08 Ma (2σ) for biotite separates from an alkali pyroxenite (Basu et al., 1993), correspond to Deccan volcanism. Early Cretaceous magmatism is also identified at Sarnu-Dandali from stratigraphic relationships (Bladon et al., 2015a). The Sarnu-Dandali complex is a therefore a polychronous, periodically rejuvenated alkaline igneous centre, much like the Mundwara complex, both of which show a remarkable parallel evolution from the Early to the Late Cretaceous, and together extend the record of Indo-Madagascar flood basalt volcanism to northwestern India, 2000 km from its known remnants in southern India. Additional equivalents buried under the vast Deccan Traps are highly likely.

Supplementary data to this article can be found online at http://dx.doi.org/10.1016/j.lithos.2017.05.005.

Acknowledgements

Field work was supported by the Industrial Research and Consultancy Centre (IRCC), IIT Bombay (Young Investigator Award grant 09YIA001 to Sheth). Pande acknowledges Grant No. IR/S4/ESF-04/2003 from the Department of Science and Technology (DST, Govt. of India) towards the development of the IIT Bombay—DST National Facility for $^{40}Ar/^{39}Ar$ Geo-thermochronology. He also thanks the IRCC, IIT Bombay, for maintenance support to the Facility (grant 15IRCCCF04). Vijayan was supported by a Ph.D. Scholarship from the University Grants Commission (U.G.C., Govt. of India). Ciro Cucciniello thanks Marcello Serracino for his patient and skillful help with the electron microprobe, Sergio Bravi for the preparation of thin sections, Michele Lustrino for technical support, and Leone Melluso for helpful discussions. Funds for the WDS analyses were provided by the "Fondi per la Ricerca Dipartimentale 2016" to Ciro Cucciniello.

We thank V. Yatheesh for enlightening discussions and for use of his continental reconstructions (Fig. 1 of this paper). The paper was improved by constructively critical reviews and comments from Greg Shellnutt, an anonymous referee, and the editor Sun-Lin Chung.

References

Ajay, K.K., Chaubey, A.K., Krishna, K.S., Gopala Rao, D., Sar, D., 2010. Seaward dipping reflectors along the SW continental margin of India: evidence for volcanic passive margin. Journal of Earth System Science 119, 803–813.

Ashwal, L.D., Solanki, A.M., Pandit, M.K., Corfu, F., Hendriks, B.W.H., Burke, K., Torsvik, T.H., 2013. Geochronology and geochemistry of Neoproterozoic Mt. Abu granitoids, NW India: regional correlation and implications for Rodinia palaeogeography. Precambrian Research 236, 265–281.

Ashwal, L.D., Wiedenbeck, M., Torsvik, T.H., 2017. Archaean zircons in Miocene oceanic hotspot rocks establish ancient continental crust beneath Mauritius. Nature Communications 8:14086. http://dx.doi.org/10.1038/ncomms14806.

Bailey, D.K., 1992. Episodic alkaline igneous activity across Africa: implications for the causes of continental break-up. In: Storey, B.C., Alabaster, T., Pankhurst, R.J. (Eds.), Magmatism and the Causes of Continental Break-up. Geol. Soc. Lond. Spec. Publ 68, pp. 91–98.

Bailey, D.K., Woolley, A.R., 2005. Repeated, synchronous magmatism within Africa: timing, magnetic reversals, and global Tectonics. In: Foulger, G.R., Natland, J.H., Presnall, D.C., Anderson, D.L. (Eds.), Plates, Plumes and Paradigms. Geol. Soc. Am. Spec. Pap 388, pp. 365–377.

Baksi, A.K., 2007. A quantitative tool for detecting alteration in undisturbed rocks and minerals – I: Water, chemical weathering, and atmospheric argon. In: Foulger, G.R., Jurdy, D.M. (Eds.), Plates, Plumes, and Planetary Processes. Geol. Soc. Am. Spec. Pap Vol. 430, pp. 285–304.

Baksi, A.R., 2014. The Deccan Trap – Cretaceous-Palaeogene boundary connection: new $^{40}Ar/^{39}Ar$ ages and critical assessement of existing argon data pertinent to this hypothesis. In: Sheth, H.C., Vanderkluysen, L. (Eds.), Flood Basalts of Asia. J. Asian Earth Sci 84, pp. 9–23.

Barker, D.S., 1974. Alkaline rocks of North America. In: Sorensen, H. (Ed.), The Alkaline Rocks. Wiley, London, pp. 150–171.

Basu, A.R., Renne, P.R., Das Gupta, D.K., Teichmann, F., Poreda, R.J., 1993. Early and late alkali pulses and a high ^{3}He plume origin for the Deccan flood basalts. Science 261, 902–906.

Beane, J.E., Turner, C.A., Hooper, P.R., Subbarao, K.V., Walsh, J.N., 1986. Stratigraphy, composition and form of the Deccan basalts, Western Ghats, India. Bulletin of Volcanology 48, 61–83.

Bhattacharya, G.C., Chaubey, A.K., 2001. Western Indian Ocean – A Glimpse of the tectonic scenario. In: Sengupta, R., Desa, E. (Eds.), The Indian Ocean – A Perspective. Oxford & IBH Publ. Co. Ltd., pp. 691–729.

Bhattacharya, G.C., Yatheesh, V., 2015. Plate-tectonic evolution of the deep ocean basins adjoining the western continental margin of India – a proposed model for the early opening scenario. In: Mukherjee, S. (Ed.), Petroleum Geoscience: Indian Contexts. Springer, pp. 1–61.

Bhushan, S.K., Chandrasekaran, V., 2002. Geology and Geochemistry of the Magmatic Rocks of the Malani Igneous Suite and Tertiary Alkaline Province of Western Rajasthan. Geological Survey of India 126 (179 pp.).

Bladon, A.J., Burley, S.D., Clarke, S.M., Beaumont, H., 2015a. Geology and regional significance of the Sarnoo Hills, eastern rift margin of the Barmer Basin, NW India. Basin Research 27, 636–655.

Bladon, A.J., Clarke, S.M., Burley, S.D., 2015b. Complex rift geometries resulting from inheritance of pre-existing structures: insights and regional implications from the Barmer Basin rift. Journal of Structural Geology 71, 136–154.

Cande, S.C., Kent, D.V., 1995. Revised calibration of the geomagnetic polarity timescale for the Late Cretaceous and Cenozoic. Journal of Geophysical Research 100, 6093–6095.

Chalapathi Rao, N.V., Dongre, A., Wu, F.-Y., Lehmann, B., 2016. A Late Cretaceous (ca. 90 Ma) kimberlite event in southern India: implication for sub-continental lithospheric mantle evolution and diamond exploration. Gondwana Research 35, 378–389.

Chaubey, A.K., Dyment, J., Bhattacharya, G.C., Royer, J.Y., Srinivas, K., Yatheesh, V., 2002. Paleogene magnetic isochrons and palaeo-propagators in the Arabian and Eastern Somali Basins, NW Indian Ocean. In: Clift, P.D., Croon, D., Gaedicke, C., Craig, J. (Eds.), The Tectonic and Climatic Evolution of the Arabian Sea Region. Geol. Soc. Lond. Spec. Pap 195, pp. 71–85.

Collier, J.S., Sansom, V., Ishizuka, O., Taylor, R.N., Minshull, T.A., Whitmarsh, R.B., 2008. Age of Seychelles-India break-up. Earth and Planetary Science Letters 272, 264–277.

Cucciniello, C., Demonterova, E.I., Sheth, H., Pande, K., Vijayan, A., 2015. $^{40}Ar/^{39}Ar$ geochronology and geochemistry of the Central Saurashtra mafic dyke swarm: insights into magmatic evolution, magma transport, and dyke-flow relationships in the northwestern Deccan Traps. Bulletin of Volcanology 77 (45):1–19. http://dx.doi.org/10.1007/s00445-015-0932-0.

Cucciniello, C., Langone, A., Melluso, L., Morra, V., Mahoney, J.J., Meisel, T., Tiepolo, M., 2010. U-Pb ages, Pb-Os isotopes ratios, and platinum-group element (PGE) composition of the West-Central Madagascar flood basalt province. Journal of Geology 118, 523–541.

Cucciniello, C., Melluso, L., Jourdan, F., Mahoney, J.J., Meisel, T., Morra, V., 2013. ^{40}Ar-^{39}Ar ages and isotope geochemistry of Cretaceous basalts in northern Madagascar: refining eruption ages, extent of crustal contamination and parental magmas in a flood basalt province. Geological Magazine 150:1–17. http://dx.doi.org/10.1017/S0016756812000088.

Devey, C.W., Stephens, W.E., 1992. Deccan-related magmatism west of the Seychelles-India rift. In: Storey, B.C., Alabaster, T., Pankhurst, R.J. (Eds.), Magmatism and the Causes of Continental Break-up. Geol. Soc. Lond. Spec. Publ 68, pp. 271–291.

Dolson, J., Burley, S.D., Sunder, V.R., Kothari, V., Naidu, B., Whiteley, N.P., Farrimond, P., Taylor, A., Direen, N., Ananthakrishnan, B., 2015. The discovery of the Barmer Basin, Rajasthan, India, and its petroleum geology. American Association of Petroleum Geologists Bulletin 99, 433–465.

Finkelstein, J., 2010. The Petrogenesis of the Mesozoic Maningoza Suite Igneous Complexes, Central-West Madagascar. (M. Sc. Thesis). Univ. Cape Town, South Africa (203 pp.).

Ganerød, M., Torsvik, T.H., van Hinsbergen, D., Gaina, C., Corfu, F., Werner, S., Owen-Smith, T.M., Ashwal, L.D., Webb, S.J., Hendriks, B.W.H., 2011. Palaeoposition of the Seychelles

microcontinent in relation to the Deccan Traps and the Plume Generation Zone in Late Cretaceous-Early Palaeogene time. In: van Hinsbergen, D.J.J., Buiter, S.J.H., Torsvik, T.H., Gaina, C., Webb, S.J. (Eds.), The Formation and Evolution of Africa: A Synopsis of 3.8 Ga of Earth History. Geol. Soc. Lond. Spec. Publ 357, pp. 229–252.

Iwata, N., Kaneoka, I., 2000. On the relationships between the ^{40}Ar-^{39}Ar dating results and the conditions of basaltic samples. Geochemical Journal 34, 271–281.

Kent, R.W., Pringle, M.S., Müller, R.D., Saunders, A.D., Ghose, N.C., 2002. ^{40}Ar/^{39}Ar geochronology of the Rajmahal basalts, India, and their relationship to the Kerguelen plateau. Journal of Petrology 43, 1141–1153.

Kshirsagar, P.V., Sheth, H.C., Shaikh, B., 2011. Mafic alkalic magmatism in central Kachchh, India: a monogenetic volcanic field in the northwestern Deccan Traps. Bulletin of Volcanology 73, 595–612.

Kumar, Anil, Pande, K., Venkatesan, T.R., Bhaskar Rao, Y.J., 2001. The Karnataka Late Cretaceous dykes as products of the Marion hotspot at the Madagascar-India breakup event: evidence from ^{40}Ar-^{39}Ar geochronology and geochemistry. Geophysical Research Letters 28, 2715–2718.

Leake, B.E., Wolley, A.R., Arps, C.E.S., Birch, W.D., Gilbert, M.C., Grice, J.D., Hawthorne, F.C., Kato, A., Kisch, H.J., Krivovichev, V.G., Linthout, K., Laird, J., Maresch, W.V., Nickel, E.H., Rock, N.M.S., Schumacher, J.C., Smith, D.C., Stephenson, N.C.N., Ungaretti, L., Whittaker, E.J.W., Youzhi, G., 1997. Nomenclature of amphiboles: report of the Subcommittee on Anphiboles of the International Mineralogical Association Commission on New Minerals and Mineral Names. European Journal of Mineralogy 9, 623–651.

Lepage, L.D., 2003. ILMAT: an Excel worksheet for ilmenite–magnetite geothermometry and geobarometry. Computational Geosciences 29, 673–678.

Ludwig, K.R., 2012. Isoplot/Ex, v. 3.75. Berkeley Geochronol. Center Spec. Publ. No. 5. Berkeley Geochronology Center.

Mahoney, J.J., Nicollet, C., Dupuy, C., 1991. Madagascar basalts: tracking oceanic and continental sources. Earth and Planetary Science Letters 104, 350–363.

McDougall, I., Harrison, T.M., 1999. Geochronology and Thermochronology by the ^{40}Ar/^{39}Ar Method. Oxford Univ. Press, Oxford.

Melluso, L., Morra, V., Brotzu, P., Franciosi, L., Petteruti Lieberknecht, A.M., Bennio, L., 2003. Geochemical provinciality in the Cretaceous magmatism of northern Madagascar, and mantle source implications. Journal of the Geological Society of London 160, 477–488.

Melluso, L., Morra, V., Brotzu, P., Tommasini, S., Renna, M.R., Duncan, R.A., Franciosi, L., d'Amelio, F., 2005. Geochronology and petrogenesis of the Cretaceous Antampombato-Ambatovy complex and associated dyke swarm, Madagascar. Journal of Petrology 46, 1963–1996.

Melluso, L., Sethna, S.F., 2011. Mineral compositions in the Deccan igneous rocks of India: an overview. In: Ray, J., Sen, G., Ghosh, B. (Eds.), Topics in Igneous Petrology. Springer, Heidelberg, pp. 135–160.

Melluso, L., Sheth, H.C., Mahoney, J.J., Morra, V., Petrone, C., Storey, M., 2009. Correlations between silicic volcanic rocks of the St. Mary's Islands (southwestern India) and eastern Madagascar: implications for Late Cretaceous India-Madagascar reconstructions. Journal of the Geological Society of London 166, 283–294.

Middlemost, E.A.K., 1989. Iron oxidation ratios, norms and the classification of volcanic rocks. Chemical Geology 77, 19–26.

Mukosi, N.C., 2012. Petrogenesis of the Ambohiby Complex, Madagascar and the Role of Marion Hotspot Plume. (M.Sc. thesis). Stellenbosch Univ., South Africa (126 pp.).

Norton, I.O., Sclater, J.G., 1979. A model for the evolution of the Indian Ocean and the breakup of Gondwanaland. Journal of Geophysical Research 84, 6803–6830.

Owen-Smith, T.M., Ashwal, L.D., Torsvik, T.H., Ganerød, M., Nebel, O., Webb, S.J., Werner, S.C., 2013. Seychelles alkaline suite records the culmination of Deccan Traps continental flood volcanism. Lithos 182-183, 33–47.

Pande, K., Cucciniello, C., Sheth, H., Vijayan, A., Sharma, K.K., Purohit, R., Jagadeesan, K.C., Shinde, S., 2017. Polychronous (Early Cretaceous to Palaeogene) emplacement of the Mundwara alkaline complex, Rajasthan, India: ^{40}Ar/^{39}Ar geochronology, petrochemistry and geodynamics. International Journal of Earth Sciences (in press). 10.1007/s00531-016-1362-8.

Pande, K., Sheth, H.C., Bhutani, R., 2001. ^{40}Ar-^{39}Ar age of the St. Mary's Islands volcanics, southern India: record of India-Madagascar breakup on the Indian subcontinent. Earth and Planetary Science Letters 193, 39–46.

Pouchou, J.L., Pichoir, F., 1984. A new model for quantitative X-ray microanalysis. I. Application to the analysis of homogeneous samples. Recherche Aerospatiale 3, 167–192.

Radhakrishna, T., Joseph, M., 2012. Geochemistry and palaeomagnetism of Late Cretaceous mafic dykes in Kerala, southwest coast of India in relation to large igneous provinces and mantle plumes in the Indian Ocean region. Geological Society of America Bulletin 124, 240–255.

Ram Mohan, M., Shaji, E., Satyanarayan, M., Santosh, M., Tsunogae, T., Yang, Q.-Y., Dhanil Dev, S.G., 2016. The Ezhimala igneous complex, southern India: possible imprint of Late Cretaceous magmatism within rift setting associated with India-Madagascar separation. Journal of Asian Earth Sciences 121, 56–71.

Rathore, S.S., Venkatesan, T.R., Srivastava, R.K., 1996a. Mundwara alkali igneous complex, Rajasthan, India: chronology and Sr isotope characteristics. Journal of the Geological Society of India 48, 517–528.

Rathore, S.S., Venkatesan, T.R., Srivastava, R.K., 1996b. Rb–Sr and Ar–Ar systematics of Malani volcanic rocks of southwest Rajasthan: evidence for a younger postcrystallization thermal event. Proceedings of the Indian Academy of Sciences (Earth and Planetary Sciences) 115, 131–141.

Rathore, S.S., Venkatesan, T.R., Srivastava, R.K., 1999. Rb–Sr isotope dating of Neoproterozoic (Malani Group) magmatism from south-west Rajasthan, India: evidence of younger Pan-African thermal event from ^{40}Ar-^{39}Ar studies. Gondwana Research 2, 271–281.

Reeves, C., 2014. The position of Madagascar within Gondwana and its movements during Gondwana dispersal. Journal of African Earth Sciences 94, 45–57.

Renne, P.R., Swisher, C.C., Deino, A.L., Karner, D.B., Owens, T.L., DePaolo, D.J., 1998. Intercalibration of standards, absolute ages and uncertainties in ^{40}Ar/^{39}Ar dating. Chemical Geology 145, 117–152.

Royer, J.Y., Chaubey, A.K., Dyment, J., Bhattacharya, G.C., Srinivas, K., Yatheesh, V., Ramprasad, T., 2002. Paleogene plate tectonic evolution of the Arabian and Eastern Somali basins. In: Clift, P.D., Croon, D., Gaedicke, C., Craig, J. (Eds.), The Tectonic and Climatic Evolution of the Arabian Sea Region. Geol. Soc. Lond. Spec. Publ 195, pp. 7–23.

Sen, A., Pande, K., Sheth, H.C., Sharma, K.K., Sarkar, S., Dayal, A.M., Mistry, H., 2013. An Ediacaran-Cambrian thermal imprint in Rajasthan, western India: evidence from ^{40}Ar-^{39}Ar geochronology of the Sindreth volcanics. Journal of Earth System Science 122, 1477–1493.

Sharma, K.K., 2007. K-T magmatism and basin tectonism in western Rajasthan, India, results from extensional tectonics and not from Réunion plume activity. In: Foulger, G.R., Jurdy, D.M. (Eds.), Plates, Plumes, and Planetary Processes. Geol. Soc. Am. Spec. Pap 430, pp. 775–784.

Shellnutt, J.G., Lee, T.-Y., Chiu, H.-Y., Lee, Y.-H., Wong, J., 2015. Evidence of Middle Jurassic magmatism within the Seychelles microcontinent: implications for the breakup of Gondwana. Geophysical Research Letters 42, 10207–10215.

Shellnutt, J.G., Yeh, M.-W., Suga, K., Lee, T.-Y., Lee, H.-Y., Lin, T.-H., 2017. Temporal and structural evolution of the Early Palaeogene rocks of the Seychelles microcontinent. Scientific Reports 7:41598. http://dx.doi.org/10.1038/s41598-017-0024-y.

Sheth, H.C., Pande, K., 2014. Geological and ^{40}Ar/^{39}Ar age constraints on late-stage Deccan rhyolitic volcanism, inter-volcanic sedimentation, and the Panvel flexure from the Dongri area, Mumbai. In: Sheth, H.C., Vanderkluysen, L. (Eds.), Flood Basalts of Asia. J. Asian Earth Sci 84, pp. 167–175.

Sheth, H.C., Pande, K., Bhutani, R., 2001. ^{40}Ar-^{39}Ar ages of Bombay trachytes: evidence for a Palaeocene phase of Deccan volcanism. Geophysical Research Letters 28, 3513–3516.

Srivastava, R.K., 1989. Alkaline and peralkaline rocks of Rajasthan. In: Leelanandam, C. (Ed.), Alkaline Rocks. Geol. Soc. Ind. Mem 15, pp. 3–24.

Steiger, R.H., Jager, E., 1977. Subcommission on geochronology; Convention on the use of decay constants in geo- and cosmochronology. Earth and Planetary Science Letters 36, 359–362.

Storetvedt, K.M., Mitchell, J.G., Abranches, M.C., Maaloe, S., Robin, G., 1992. The coast-parallel dolerite dykes of east Madagascar: age of intrusion, remagnetization and tectonic aspects. Journal of African Earth Sciences 15, 237–249.

Storey, M., Mahoney, J.J., Saunders, A.D., 1997. Cretaceous basalts in Madagascar and the transition between plume and continental lithosphere mantle sources. In: Mahoney, J.J., Coffin, M.F. (Eds.), Large Igneous Provinces: Continenntal, Oceanic, and Planetary Flood Volcanism. Am. Geophys. Union Geophys. Monogr 100, pp. 95–122.

Storey, M., Mahoney, J.J., Saunders, A.D., Duncan, R.A., Kelley, S.P., Coffin, M.F., 1995. Timing of hotspot-related volcanism and the breakup of Madagascar and India. Science 267, 852–855.

Torsvik, T.H., Tucker, R.D., Ashwal, L.D., Carter, L.M., Jamtveit, B., Vidyadharan, K.T., Venkataramana, P., 2000. Late Cretaceous India-Madagascar fit and timing of breakup related magmatism. Terra Nova 12, 220–224.

Torsvik, T.H., Tucker, R.D., Ashwal, L.D., Eide, E.A., Rakotosolofo, N.A., de Wit, M.J., 1998. Late Cretaceous magmatism in Madagascar: palaeomagnetic evidence for a stationary Marion hotspot. Earth and Planetary Science Letters 164, 221–232.

Valsangkar, A.B., Radhakrishnamurthy, C., Subbarao, K.V., Beckinsale, R.D., 1981. Paleomagnetism and potassium-argon age studies of acid igneous rocks from the St. Mary Islands. In: Subbarao, K.V., Sukheswala, R.N. (Eds.), Deccan Volcanism. Geol. Soc. Ind. Mem 3, pp. 265–275.

Verma, S.P., Torres-Alvarado, I.S., Sotelo-Rodriguez, Z.T., 2002. SINCLAS: standard igneous norm and volcanic rock classification system. Computational Geosciences 28, 711–715.

Vijayan, A., Sheth, H., Sharma, K.K., 2016. Tectonic significance of dykes in the Sarnu-Dandali alkaline complex, Rajasthan, northwestern Deccan Traps. Geoscience Frontiers 7, 783–791.

Viladkar, S.G., 2015. Preliminary investigation of Ba-rich sanidine in phonolites of Badmer, Rajasthan. Journal of the Geological Society of India 86, 300–304.

Yatheesh, V., 2007. A Study of Tectonic Elements of the Western Continental Margin of India and Adjoining Ocean Basins to Understand the Early Opening of the Arabian Sea. (Ph.D. Thesis). Goa Univ., Goa (212 pp.).

Yatheesh, V., Bhattacharya, G.C., Mahender, K., 2006. The terrace like feature in the mid-continental slope region off Trivandrum and a plausible model for India-Madagascar juxtaposition in immediate pre-drift scenario. Gondwana Research 10, 179–185.

Zellmer, G.F., Sheth, H.C., Iizuka, Y., Lai, Y.-J., 2012. Remobilization of granitoid rocks through mafic recharge: evidence from basalt-trachyte mingling and hybridization in the Manori-Gorai area, Mumbai, Deccan Traps. Bulletin of Volcanology 74, 47–66.